THE JOURNAL OF PHYSICAL CHEMISTRY C LETTERS

2008, *112,* 20123–20125
Published on Web 12/04/2008

Chirality-Dependent Raman Frequency Variation of Single-Walled Carbon Nanotubes under Uniaxial Strain

Bo Gao, Lai Jiang, Xi Ling, Jin Zhang,* and Zhongfan Liu*

Beijing National Laboratory for Molecular Sciences (BNLMS), Key Laboratory for the Physics and Chemistry of Nanodevices, State Key Laboratory for Structural Chemistry of Unstable and Stable Species, College of Chemistry and Molecular Engineering, Peking University, Beijing 100871, P. R. China

Received: October 22, 2008; Revised Manuscript Received: November 18, 2008

By using a homemade setup, the length of uniaxial strained single-walled carbon nanotubes (SWNTs) was directly measured by scanning electron microscopy (SEM), and quantitative relations between uniaxial strain and Raman frequency were obtained. It was found that RBM frequency was not affected, but *G*-band frequency variation was diameter and chirality-dependent under uniaxial strain. The *G*-band frequency shift rate increased with diameter increasing and chiral angel decreasing. Also G^+ and G^- frequency shift rates were related to chiral angle due to chirality-dependent C−C bonds elongation. A surprising finding that intermediate frequency mode (IFM) frequency upshifted with uniaxial strain increasing indicates that lattice transformation needs to be considered in phonon properties under uniaxial strain. These studies provide valuable information about geometric structure variation of SWNTs under uniaxial strain.

Introduction

The electronic structure and chemical and physical properties of single-walled carbon nanotubes (SWNTs) uniquely depend on their chiral indices (*n*, *m*).[1,2] This also applies to their response to uniaxial strain, which is a hot topic in recent studies on SWNTs. Theoretical and experimental studies both revealed that the electronic structure of SWNTs can change significantly with uniaxial strain and follows the family pattern.[3−9] A recent experimental study by Huang et al.[7] directly measured the uniaxial strain-induced changes in the electronic structure of SWNTs and presented a revised relationship, which has an implication in the analysis of the coupling between the electronic system and any long-wavelength acoustic phonon.

Resonant Raman spectroscopy of SWNTs, which is closely related to their chiral indices, is a powerful tool in probing the geometrical structure[1] and structure transformation[10] in SWNTs. Theoretical calculations show that radial breathing mode (RBM) did not shift, but tangential *G*-band linearly downshifted with uniaxial strain increasing.[11,12] There have also been several experimental studies concerning the uniaxial strain induced Raman frequency variation of SWNTs.[10,13−16] However, due to indirect measurement and low precision of uniaxial strain, different relations between uniaxial strain and Raman frequency were given, and the dependence on chirality was not yet observed.

In this paper, the length of uniaxial strained SWNTs was directly measured by scanning electron microscopy (SEM) to obtain quantitative relations between uniaxial strain and Raman frequency, and thus the dependence of Raman frequency variation on chirality was first reported. New findings on Raman modes, including *G*-band, IFM and *D*-band, indicate lattice transformation needs to be considered in phonon properties under uniaxial strain.

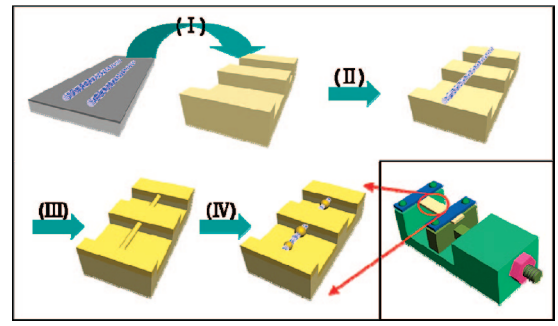

Figure 1. Schematic figure for preparing samples. (I) SWNTs and PDMS with trenches were prepared. (II) SWNTs were transferred onto PDMS surface by dry method. (III) 12 nm thick gold films were deposited onto PDMS surface. (IV) Gold particles were prepared by laser heating. Inset: homemade stretching setup. By controlling the screw rotation, the length of PDMS and hence the length of suspended SWNTs were controlled.

Experimental Section

The experiment was carried out using a homemade stretching setup (see inset of Figure 1). By rotating a screw at the step of 30°, flexible polydimethylsiloxane (PDMS) was stretched and then uniaxial strain was introduced into suspended SWNTs gradually. The sample was prepared as follows (see Figure 1). SWNTs were grown on a SiO_2/Si substrate by catalytic chemical vapor decomposition (CVD) of ethanol.[17] PDMS with trenches was prepared by pouring DMS on Si with patterns and heat curing. By pressing the SiO_2/Si substrate against flexible PDMS with trenches, some SWNTs were transferred to PDMS. Since the trench was 2.5 μm deep and 4−8 μm wide, most SWNTs

* To whom correspondence should be addressed. Tel & Fax: 86-10-6275-7157. E-mail: jinzhang@pku.edu.cn.

10.1021/jp809374j CCC: $40.75

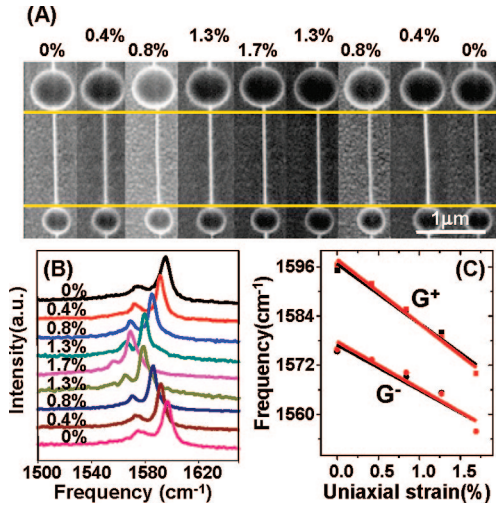

Figure 2. (A) SEM image, (B) *G*-band spectra of (18, 5) SWNT when uniaxial strain first increases from 0% to 1.7% and then decreases to 0%. (C) G^+ and G^- frequencies variation as a function of uniaxial strain. Black (red) dots and lines correspond to the increase (decrease) of uniaxial strain. Lines are linearly fitted from dots which are obtained by Lorentzian fitting.

were suspended in the trench. About 12 nm thick gold films were deposited onto the PDMS and SWNTs. Deposited gold films on PDMS could hold SWNTs in place and prevent suspended SWNTs slack. By laser heating at 100% of laser intensity (7 mW), gold films on PDMS and SWNTs evaporated and then recrystallized as gold particles on suspended SWNTs. These gold particles on suspended SWNTs were reference marks to measure the length of SWNTs directly and precisely, which is also a good prototype for surface enhanced Raman scattering (SERS) effect. At each uniaxial strain Raman spectral characterization (633 nm He−Ne laser) at 50% of laser intensity and subsequent SEM measurement (resolution better than 5 nm at 1 kV) were preformed separately.

Results and Discussion

Figure 2A shows the SEM image of a suspended (18, 5) SWNT, uniaxial strain of which first increase and then decrease by stretching and relaxing PDMS. The length between two gold particles can be directly measured on the SEM image. It can be seen that the length between two gold particles first increases and then decreases linearly. Due to high resolution of SEM, the length of uniaxial strained SWNTs can be precisely measured and hence their strain can be accurately calculated. Raman spectral characterization shows that RBM does not shift (see Figure S1 in Supporting Information), but *G*-band (both G^+ and G^-) first downshifts and then upshifts to the original frequency (see Figure 2B). Figure 2C shows the *G*-band frequencies (ω_{G^+} and ω_{G^-}) as a function of uniaxial strain. It can be found that *G*-band frequencies are linearly proportional to uniaxial strain, satisfying the relations $\omega_{G^+}(\mathrm{cm}^{-1}) = 1596.79-14.59\epsilon$ and $\omega_{G^-}(\mathrm{cm}^{-1}) = 1577.00-11.00\epsilon$ for G^+ and G^- frequencies respectively. Here ϵ is the uniaxial strain, and is calculated by $(L - L_0)/L_0$ (L_0 and L are the unstrained and strained length respectively). The shift rate of G^+ is a little larger than that of G^-. It is noted that *G*-band frequencies overlap at the same strain during stretching and relaxing, which indicates that there is no slippage between SWNTs and PDMS during experiment.

As shown in Figure 3, for (7, 5) SWNT, similar results are observed. When uniaxial strain increases from 0 to 7.1%, RBM

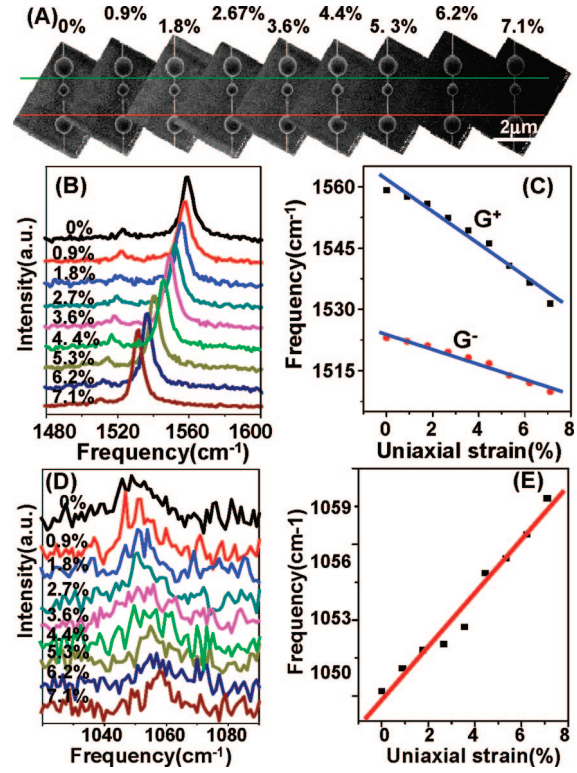

Figure 3. (A) SEM image, (B) *G*-band spectra and (C) IFM spectra of (7, 5) SWNT when uniaxial strain increase from 0% to 7.1%. (D) G^+, G^- and (E) IFM frequencies as a function of uniaxial strain; lines are linearly fitted from experimental data which are obtained by Lorentzian fitting.

TABLE 1: Uniaxial Strain Induced Raman Frequency Variation of 7 Individual SWNTs[a]

RBM (cm^{-1})	(n,m)	d (nm)	θ (°)	G^+ (cm^{-1}/%)	G^- (cm^{-1}/%)
310	(6,5)	0.76	27.00	−3.97	N/A
281	(7,5)	0.83	24.50	−3.95	−1.89
213	(11,5)	1.13	17.78	−6.50	N/A
177	(14,5)	1.35	14.70	−6.43	N/A
171	(13,7)	1.40	20.17	−13.06	−11.80
146	(18,5)	1.66	11.93	−14.59	−11.00
N/A	N/A	N/A	N/A	−19.25	−31.02

[a] d: diameter; θ: chiral angle; (n, m) are assigned from RBM frequency; d and θ are calculated from (n, m). N/A means that the peaks are not observed.

does not shift (see Figure S2 in Supporting Information), but both G^+ and G^- downshift linearly at a rate of -3.95 cm^{-1}/% and -1.89 cm^{-1}/% (see Table 1). The shift rate of G^+ is much larger than that of G^-, about twice as that of G^-. Hence, as shown in Figure 3B, the peaks of G^+ and G^- are closer and closer with uniaxial strain increasing. The difference in relative shift rate between G^+ and G^- is probably because the unit cells of graphene arrange along different directions relative to the SWNTs axis.

Due to SERS effect of gold particles on SWNTs, one intermediate frequency mode (IFM) is luckily observed (see Figure 3D). What makes surprise is that IFM frequency (ω_{IFM}) upshifts linearly with uniaxial strain increasing, satisfying the relations $\omega_{\mathrm{IFM}}(\mathrm{cm}^{-1}) = 1049.84 + 1.06\epsilon$. This is the first time that IFM frequency shifts under uniaxial strain is observed and the shift trend is opposite to other Raman modes. Previous studies attributed the uniaxial strain induced downshift of Raman modes to elongation of C−C bonds, which weakened C−C bonds.[11,15] Obviously, this explanation cannot apply to IFM. It

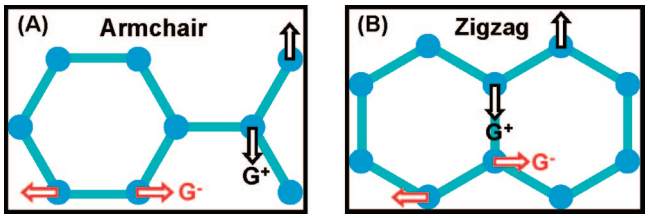

Figure 4. Schematic figures for *G*-band vibrations in (A) armchair and (B) zigzag SWNTs.

is known that IFMs relate to the double resonance process and are originated from the combination of two phonon modes, one optical and one acoustic.[18] It is speculated that uniaxial strain induced lattice transformation needs to be considered when some complicated Raman scattering processes are involved, which may also be a minor factor in the shift of *G*-band frequency.

As shown in Table 1, we have measured Raman spectra on seven different SWNTs. Under uniaxial strain all RBM does not shift, but *G*-band downshifts and the downshift rates range from -1.89 cm^{-1}/% to -31.02 cm^{-1}/%. In previous studies, by stretching SWNTs/epoxy composites, Cooper et al.[13] have measured *G*′-band frequency and got the shift rate of -13.0 ± 3.8 cm^{-1}/%, in which the elongating rate of composites was used as uniaxial strain of SWNTs. Moreover, slippage tended to occur during the stretching process. The indirect measurement of uniaxial strain and the possible slippage probably bring errors to the shift rate. By AFM tip manipulation, Cronin et al.[15] stretched on-substrate SWNTs two ends of which were held by metal electrodes to avoid slippage. Their shift rate range from -6 cm^{-1}/% to -25 cm^{-1}/%. However, in their experiment uniaxial strain was not uniform along SWNTs and the length of curved SWNTs was difficult to measure, which makes the calculation of shift rate less accurate. In our experiment, suspended SWNTs are easily measured by SEM and can ensure the uniform distribution of uniaxial strain. Furthermore, stretching and relaxing experiment and repetitious measurement experiment (see Figure S3 in Supporting Information) indicate no slippage occurring between SWNTs and PDMS.

Direct length measurement of uniaxial strained SWNTs by SEM and quantitative relations between Raman frequency and uniaxial strain facilitate us to know the dependence of Raman frequency of SWNTs on chirality. From Table 1, it can be seen that, for (7, 5) SWNT, the shift rate of G^+ is only -3.95 cm^{-1}/%, while another SWNT as large as -19.25 cm^{-1}/%. Among the six SWNTs with RBM, the shift rate of G^+ increases with diameter increasing and chiral angle decreasing. It is thought that diameter and chiral angle may play roles together. So far it is not clear how diameter and chiral angle relate to different shift rate in principle.

From Table 1, it can also be seen that, for (7, 5) SWNT, the shift rate of G^+ is far larger than that of G^-; for (13, 7) and (18, 5) SWNTs, the shift rate of G^+ is a little larger than that of G^-; for another SWNT, the shift rate of G^+ is far smaller than that of G^-. The relative shift rate between G^+ and G^- is related to chiral angle.[15] As we know, G^+ and G^- correspond to axial and circumferential vibrations respectively. For armchair SWNTs or SWNTs close to armchair (e.g., (7, 5) SWNT), G^--dependent C−C bonds are perpendicular to the axial of SWNTs (see Figure 4A). Therefore G^- is less affected than G^+ for armchair SWNTs. As shown in Figure 4B, it is reversed for zigzag SWNTs. It is the chirality-dependent C−C bonds elongation that causes differences in the relative shift rate between G^+ and G^-.

It is noted that there are no *D*-band occurring even 7% uniaxial strain for (7, 5) SWNT (see Figure S4 in Supporting Information). It is known that *D*-band is centered at ∼1300 cm^{-1} and is originated from disorders in SWNTs, such as dangling bond, 5−7 ring, sp^3 hybridization or edge effect.[18] *D*-band is not observed in all uniaxial strained SWNTs. Our observation is not consistent with Lee's finding:[13] in some uniaxial strained SWNTs a small and sharp *D*-band occurred at a very small uniaxial strain, e.g., 0.004%. No occurrence of *D*-band means that SWNTs possess excellent elastic property and uniaxial strain only induces lattice transformation which can be recovered when uniaxial strain is relaxed.

Conclusion

In conclusion, we measured the quantitative relations between Raman frequency and uniaxial strain of SWNTs, and found that the variation of Raman frequency was strongly dependent on their chirality. This finding can help us know geometric structure variation of SWNTs under uniaxial strain. Another direct implication of this study is in the analysis the SWNTs enhanced composites. Precise relations between Raman frequency and uniaxial strain can bring a simple and accurate method of characterizing uniaxial strain in the research and application of composites. Also, our study presents a novel and universal experimental scheme for the research of one-dimensional nanowires and other nanomaterials.

Acknowledgment. This work was supported by NSFC (Grants 20573002, 20673004, 20725307, and 50521201) and MOST (Grants 2006CB932701, 2006CB932403, and 2007CB936203).

Supporting Information Available: The variation of RBM (Figure S1 and S2) and *D*-band spectra (Figure S4) under uniaxial strain; *G*-band during repetitious measurement experiment (Figure S3). This material is available free of charge via the Internet at http://pubs.acs.org.

References and Notes

(1) Saito, R.; Dresselhaus, G.; Dresselhaus, M. S. *Physical Properties of Carbon Nanotubes*; Imperial College Press: London, 1992.
(2) Doyle, C. D.; Rocha, J. D. R.; Weisman, R. B.; Tour, J. M. *J. Am. Chem. Soc.* **2008**, *130*, 6795.
(3) Heyd, R.; Charlier, A.; McRae, E. *Phys. Rev. B* **1997**, *55*, 6820.
(4) Minot, E. D.; Yaish, Y.; Sazonova, V.; Park, J. Y.; Brink, M.; McEuen, P. L. *Phys. Rev. Lett.* **2003**, *90*, 156401.
(5) Souza, A. G.; Kobayashi, N.; Jiang, J.; Gruneis, A.; Saito, R.; Cronin, S. B.; Mendes, J.; Samsonidze, G. G.; Dresselhaus, G. G.; Dresselhaus, M. S. *Phys. Rev. Lett.* **2005**, *95*, 217403.
(6) Yang, L.; Han, J. *Phys. Rev. Lett.* **2000**, *85*, 154.
(7) Huang, M. Y.; Wu, Y.; Chandra, B.; Yan, H.; Shan, Y.; Heinz, T. F.; Hone, J. *Phys. Rev. Lett.* **2008**, *100*, 136803.
(8) Leeuw, T. K.; Tsyboulski, D. A.; Nikolaev, P. N.; Bachilo, S. M.; Arepalli, S.; Weisman, R. B. *Nano Lett.* **2008**, *8*, 826.
(9) Maki, H.; Sato, T.; Ishibashi, K. *nano Lett.* **2007**, *7*, 890.
(10) Duan, X. J.; Son, H. B.; Gao, B.; Zhang, J.; Wu, T. J.; Samsonidze, G. G.; Dresselhaus, M. S.; Liu, Z. F.; Kong, J. *Nano Lett.* **2007**, *7*, 2116.
(11) Wu, G.; Zhou, J.; Dong, J. M. *Phys. Rev. B* **2005**, *72*, 115411.
(12) Yang, W.; Wang, R. Z.; Yan, H. *Phys. Rev. B* **2008**, *77*, 195440.
(13) Cooper, C. A.; Young, R. J.; Halsall, M. *Composites: Part A* **2001**, *32*, 401.
(14) Cronin, S. B.; Swan, A. K.; Unlu, M. S.; Goldberg, B. B.; Dresselhaus, M. S.; Tinkham, M. *Phys. Rev. Lett.* **2004**, *93*, 167401.
(15) Cronin, S. B.; Swan, A. K.; Unlu, M. S.; Goldberg, B. B.; Dresselhaus, M. S.; Tinkham, M. *Phys. Rev. B* **2005**, *72*, 35425.
(16) Lee, S. W.; Jeong, G. H.; Campbell, E. E. B. *Nano Lett.* **2007**, *7*, 2590.
(17) Zhang, Y. Y.; Zhang, J.; Son, H. B.; Kong, J.; Liu, Z. F. *J. Am. Chem. Soc.* **2005**, *127*, 17156–17157.
(18) Dresselhaus, M. S.; Dresselhaus, G.; Saito, R.; Jorio, A. *Phys. Rep.* **2005**, *409*, 47.

JP809374J